Bull. Mater. Sci. (2020) 43:88
https://doi.org/10.1007/s12034-020-2059-y

Effect of thermal cycling on mechanical and thermal properties of basalt fibre-reinforced epoxy composites

FARZIN AZIMPOUR-SHISHEVAN[1], HAMIT AKBULUT[1] and M A MOHTADI-BONAB[2,*]

[1]Department of Mechanical Engineering, Faculty of Maragheh, Maragheh Branch, Technical and Vocational University, Tehran, Iran

[2]Department of Mechanical Engineering, University of Bonab, Velayat Highway, Bonab, Iran

*Author for correspondence (m.mohtadi@bonabu.ac.ir)

MS received 10 November 2018; accepted 19 October 2019; published online 6 March 2020

Abstract. Current study investigated the effect of thermal fatigue on mechanical and thermal properties of basalt fibre-reinforced polymer (BFRP) composites. To this, basalt fibre textiles in 2/2 twill pattern was used to fabricate BFRP composites. Thermal cycling experiment was carried out between −40 and +120°C for 20, 40, 60, 80 and 120 cycles. Moreover, dynamic mechanical analyzer (DMA) was used to evaluate the effect of thermal cycling on thermal properties of BFRPs. Moreover, we compared the extracted viscoelastic characteristics, such as storage modulus, loss modulus and loss factor curves with original thermal-treated BFRP specimens. Based on the results, thermal cycling affected the characteristics of composites in the post-curing stage due to an increase in temperature. Finally, the effect of thermal cycling on water absorption properties of BFRP composites was examined by hydrophobicity test. The results showed that tensile strength, flexural modulus and ILSS values increased with the increase in the number of cycles up to 80 cycles. In other words, an increase in the number of cycles increased the hydrophobicity of BFRP composites by decreasing the contact angles. Finally, the mechanical properties of tested composites were significantly decreased when the number of cycles reached 120. This was due to the mismatch of thermal expansion coefficient and long crack formation in the structure of composite.

Keywords. Thermal cycling; mechanical properties; thermal properties; basalt fibre; epoxy.

1. Introduction

Composite materials are widely used in industries, since they have high mechanical properties. However, their side effects, such as harmful bio-effects, have limited their applications. Recently, some researchers used inorganic fibres for composite reinforcement, because of their ecofriendly characteristics. For this reason, natural fibres such as wood, bamboo, palm, sisal, jute, hemp and coir were used in composite structure as a matrix reinforcement [1–11]. The low mechanical and thermal properties of these fibres have restricted their applications [12]. Some other factors, such as low thermal stability, poor wettability and hydrophilic nature and poor interfacial adhesion of matrix materials, are considered as the main deficiencies of such fibres [13–15]. Therefore, researchers have always been looking for a material to use as inorganic fibre with better properties in the composite structure. Basalt fibre was appeared as a novel inorganic material, which has better tensile and compressive properties than those of glass fibre [9,16–19]. Therefore, it has attracted a significant attention as a new ecofriendly brand [20]. Nontoxicity, non-combustibility, resistance to alkaline and acidic conditions and good corrosion resistance are considered as some unique properties of basalt fibre, which distinguish it from other materials [21–25]. More importantly, this fibre is cheaper than other reinforced materials such as carbon fibre. Its rich resources, easy manufacturing process and additive-free property lead to decrease the production costs [26,27]. Therefore, the demand for basalt fibre-reinforced polymer (BFRP) composites has increased in recent years in the industry, where high thermal resistance is vital. Several efforts have been made to investigate the basalt fibre response to various conditions; however, behaviour of such composites in variable temperatures has not been sufficiently studied. For instance, Wei *et al* [28] studied the tensile behaviour of basalt fibre after a chemical treatment. Lu *et al* [29] studied the effect of elevated temperatures on the mechanical properties of basalt fibres and BFRPs plate. They indicated that the tensile strength and elastic modulus of BFRPs were reduced when the ambient temperature reached over the room temperature (RT). Liu *et al* [30] investigated the mechanical properties of BFRPs in transportation systems. They fabricated BFRPs and GFRPs by hand-layup method and tested their mechanical properties. The results revealed that BFRPs and GFRPs have similar behaviour when they were subjected to mechanical loading. Botev *et al* [31] studied the mechanical and viscoelastic properties of basalt fibre-reinforced polypropylene (PP) composites. This research investigated the effect of the addition of propylene-g-maleic anhydride (PP-g-MA) to the BFRPs to enhance the interfacial interaction. The results of this research showed that the increase in the PP-g-MA percentage to modify the PP matrix leads to a higher stiffness of fabricated composite. Chandekar *et al* [32] studied the low velocity impact behaviour of homogeneous carbon, basalt and inter-ply hybrid of fibre-reinforced composites. They observed that the low velocity impact behaviour of hybrid composites had better performance than that of classic basalt fibre- and carbon fibre-reinforced composites (CFRP). Dehkordi *et al* [33] studied the low velocity impact behaviour of basalt/nylon-based intra-ply hybrid and homogeneous composites. The combination of high mechanical properties of basalt fibres with superior impact behaviour of nylon fibres was reported as the purpose of this research. The results indicated that at a low impact energy, hybridization and variation in basalt/nylon fibre content did not improve the impact performance of composite plates. Lopresto *et al* [34] evaluated the mechanical performance of BFRP composites to replace the glass fibre in the structure of composites with a better material with a higher tensile and bending properties. Zhang *et al* [35] investigated the mechanical and thermal properties of basalt fibre-reinforced polybutylene succinate composites. They fabricated composite samples with different fibre contents and evaluated their tensile, flexural and impact properties and thermal stability as well. The results of their research showed that fabricated BFRPs may be a potential choice for manufacturing of some daily commodities. Azimpour *et al* [36] hybridized basalt fibres with carbon fibre in the structure of intra-ply hybrid composite to improve the impact behaviour of CFRP. They showed that the low velocity impact behaviour of CFRPs was improved by the addition of basalt fibre to the structure of composite. Kim *et al* [37,38] examined the thermal and physical properties of epoxy composite reinforced with basalt fibre and showed that BFRPs had very high thermal properties. Liu *et al* [39] investigated the effect of thermal cycling on mechanical and thermal properties of BFRP composites. These researchers observed that BFRPs had better performance compared with other types of natural fibre-reinforced composites. In another research, Azimpour-Shishevan *et al* [40] investigated the low velocity impact behaviour of BFRPs by fabricating them. The results of their research emphasized on good impact toughness of BFRPs.

One of the important applications of BFRP composites is in marine structures [26]. These structures are continuously exposed to thermal variation during their service. The thermal variation between two levels is often referred as thermal cycling. Thermal cycling provides large thermal gradient in composite construction [39]. When the specimen is cooled from the elevated temperature to cryogenic temperature during quenching treatment, the compressive and tensile stresses are created at the interior and the surface sections, respectively [41]. Therefore, the nature of thermal stresses is compressive in the fibres and is tensile in the matrix [42].

Since various components provide different amounts of coefficient of thermal expansions (CTEs), appropriate material selection, such as component selection in the structure of composite materials, is very important. Different amounts of CTE create different strain rates and mismatch in the structure of composite during temperature variation. These conditions lead to the creation of thermal stress in the interface of composite [43–45]. Clearly, the interface between fibre and matrix is considered as an important region in the structure of composites, where stress concentration is high [46]. When temperature varies frequently, the strain rate mismatch inside the composite structure reoccurs and stress concentration increases at the interface [47]. It also creates microcracks at the interface and initiates delamination. Delamination is one of the inherent weaknesses of laminated composites, which degrades their structure. On the other hand, thermal residual stresses severely reduce the maximum load resistance of composites [48]. Moreover, tensile stress created in the matrix strongly reduces the strain to the failure of epoxy matrix [49]. In this research, we applied tensile, bending, short beam shear (SBS) and dynamic mechanical analysis (DMA) experiments to investigate the effect of temperature variation on the mechanical and thermal properties of BFRP composite materials.

2. Experimental

2.1 *Materials and specimen preparation*

We provided the required BF textiles in 2/2 twill pattern. In this pattern, fibres were weaved at 0 and 90° orientation angles (figure 1a) and identified by its diagonal parallel lines known as wales. Designated 2/2 numerator indicated fibres warp and weft thread in which a bundle of weft thread passed over two basalt warp threads. Each ply consisted of 40% basalt fibre as a reinforcement and 60% epoxy as a matrix phase. It means that 40% of composite volume is made from the fibre and the rest is made from matrix. Homogenous BFRP composites including basalt fibres as a reinforcement and epoxy as a matrix were fabricated by vacuum assisted resin infusion molding (VARIM) method (figure 1b). The wt% of SiO_2 varied between 48.8 and 50. The wt% of Al_2O_3 and MgO varied from 13.7 to 14.3 and from 5.6 to 6.1, respectively. The bulk rock FeO/MgO ratio was between 1.74 and 2 wt%. The VARIM process involved the use of a vacuum to facilitate resin flow into the fibre layup. The fibre layup included a mould tool covered by a vacuum bag. The resin was sucked from matrix container and then passed through the fibres, plies and finally, exited from the other side. The areal mass of basalt fabrics was 225 g $m^{-2} \pm 5\%$ and the thickness of fabricated composites was 2.5 mm. The size of fabricated composite plates was 700×700 cm^2. The plates were cut with water jet according to ASTM standard of reinforced plastic materials. Mechanical and physical properties of composite components are illustrated in table 1.

The epoxy used in the process was Huntsman araldite 1564 mixed with its hardener aradur 3487. The modulus of elasticity and tensile strength of the epoxy were 3300 and 92 MPa, respectively. The diameter of basalt fibre in the composite

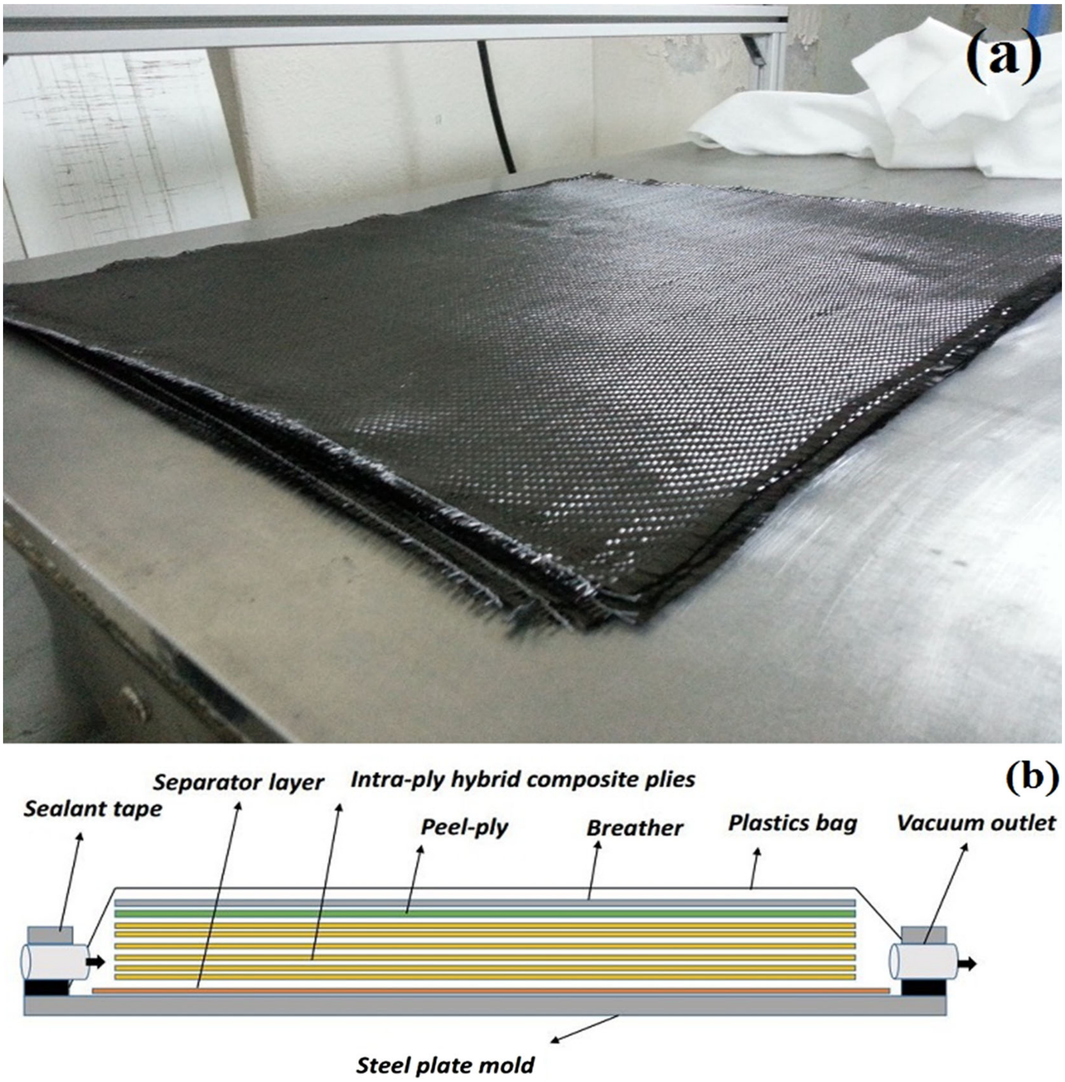

Figure 1. BFRP composites fabrication: (**a**) weaved textiles and (**b**) schematic of VARIM method.

Table 1. Mechanical and physical properties of used materials as components of composite structure.

Material	Basalt fibre	Epoxy
Density (g cm^{-3})	2.1	1.13
Modulus of elasticity (GPa)	64	3.3
Tensile strength (MPa)	4530	92
Thermal conductivity (W $m^{-1}k^{-1}$)	0.033	0.6
Coefficient of thermal expansion (1/°C) $\times 10^{-6}$	6	65

structure was 13 μm. The fabricated composites included 12 plies of 2/2 twill woven fabrics with the density of 210 g m^2. The curing process of the composites was carried out at −1 atm. pressure and 80°C temperature for 8 h. Weaved basalt fabrics and schematic of composite fabrication process (VARIM) are illustrated in figure 1b.

2.2 *Thermal cycling process*

Thermal cycling process was defined as a sequence in which the temperature increased form RT to 120°C, then decreased to −40°C and finally returned to RT. The total thermal cycling process time was 20 min. This sequence was repeated for 20, 40, 60, 80 and 120 cycles. The temperature profile of this sequence is illustrated in figure 2. We tested five samples in each process.

2.3 *Mechanical tests*

We evaluated the effect of thermal cycling on mechanical properties of BFRP composites using tensile, bending and SBS tests. We compared the tensile strength, flexural

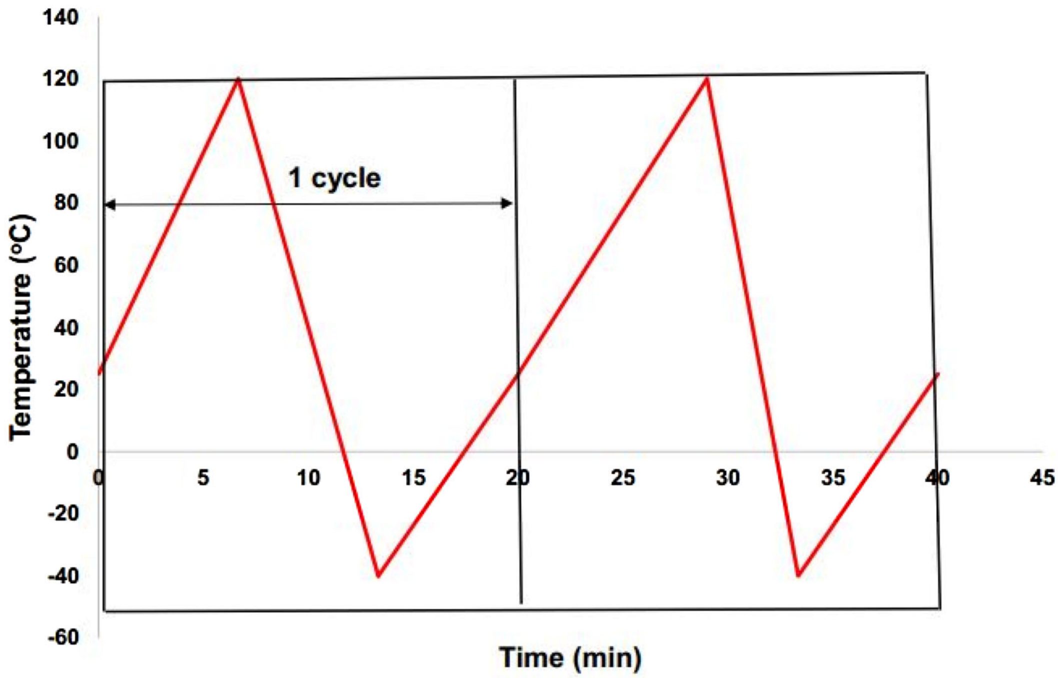

Figure 2. Temperature profile of thermal cycling process.

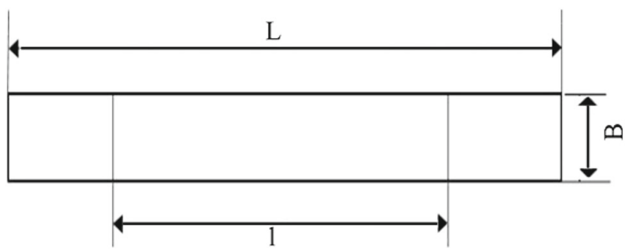

Figure 3. Geometry of mechanical test specimens.

Table 2. Dimensions of test specimens for mechanical tests.

Test	*L* (mm)	*l* (mm)	*B* (mm)
Tensile	250	150	25
Bending	130	100	15
SBS	50	40	7

modulus and ILSS of treated specimens with the original ones. We also carried out all mechanical tests at RT according to ASTM D3039 standard for tensile, ASTM D790 for bending and ASTM D2344 for SBS. The instrument crosshead speed for tensile, bending and SBS tests was 1, 1 and 1.3 mm min^{-1}, respectively. The geometry and dimensions of test specimens were illustrated in figure 3 and table 2. It is notable that in tensile test, the distance between grips was 20 cm. The distances between supporting pins for bending and SBS experiments were 12 and 3 cm, respectively.

The tensile strength, flexural modulus and flexural strength were calculated using equations (1, 2 and 3), respectively. Also, equation (4) was used for calculating ILSS by SBS test.

$$\sigma_t = \frac{P}{A}, \tag{1}$$

$$E_f = \frac{mL^3}{4Bt^3}, \tag{2}$$

$$\sigma_f = \frac{3PL}{2Bt^2}, \tag{3}$$

$$\tau = 0.75 \times \frac{P}{Bt}. \tag{4}$$

In the above equations, P is maximum load (N), A the area of crosssection, B sample's width and t its thickness. In equation (2), m is the slope of force-deflection diagram in bending test [50].

2.4 *DMA*

We carried out the DMA test for original fabricated BFRP and thermal exposure specimens using Perkin Elmer Pyris Diamond DMA instrument. This test was considered as an effective method to characterize the viscoelastic properties of composite materials. This technique was used to examine the materials viscoelastic behaviour against vibrational loads. In this method, we tested homogeneous BFRP composites under 3-point bending mode at the frequency of 1 Hz at the temperature ranging from 25 to 200°C. The maximum mechanical load and the heating rate were 18 N and 2°C min^{-1}, respectively. The mechanical loads in DMA

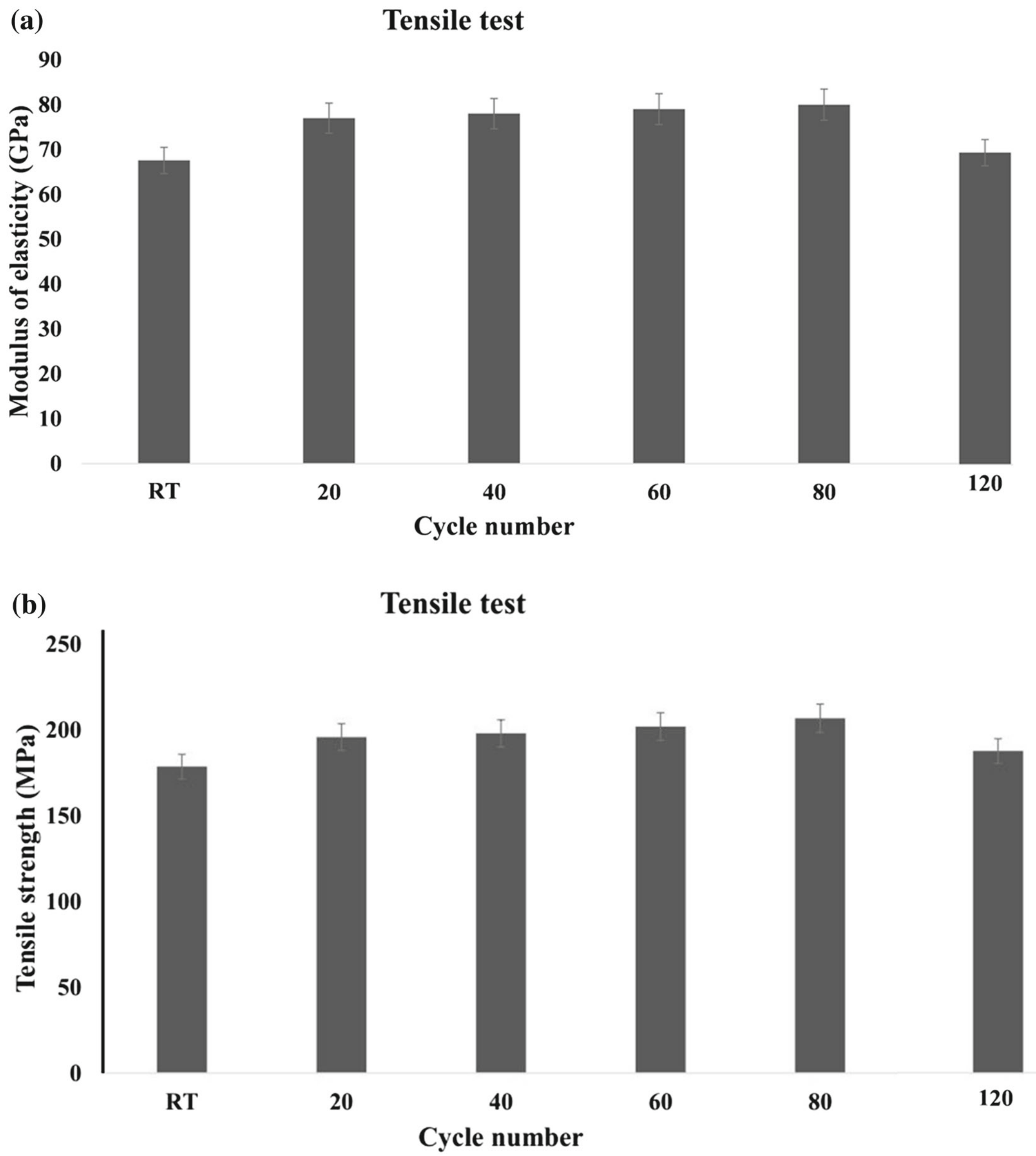

Figure 4. (**a**) Modulus of elasticity and (**b**) tensile strength of BFRP composites before and after various numbers of thermal cycling exposure.

test varied between 4 and 18 N. We also used ASTM D7028 standard for DMA test. According to this standard, dimension of the cross-section of the samples were 7×7 mm^2. The viscoelasticity properties diagrams, such as storage modulus (E') and loss modulus (E''), were plotted against temperature and measured by Pyris software. Finally, we determined the glass transition temperature of original fabricated and thermal exposure BFRP composites from tan diagram. It should be noted that the transition temperature is the temperature in which tan δ gets the maximum value.

2.5 *Hydrophobicity test*

The hydrophilic and hydrophobic natures of fabricated BFRP composite was examined before and after thermal cycling exposure using hydrophobicity test. Since BFRP composites were widely used in marine structures, it was necessary to examine their water absorption characteristics. We carried out hydrophobicity test using KSV CAM 101 goniometer and then determined the contact angle of each specimen. It is important to note that material with a contact angle (θ) higher than 90° was considered as hydrophobic type, otherwise it was from hydrophilic type.

3. Results and discussion

3.1 *Mechanical tests*

As mentioned before, the mechanical properties of original fabricated and thermal cycling exposure BFRP

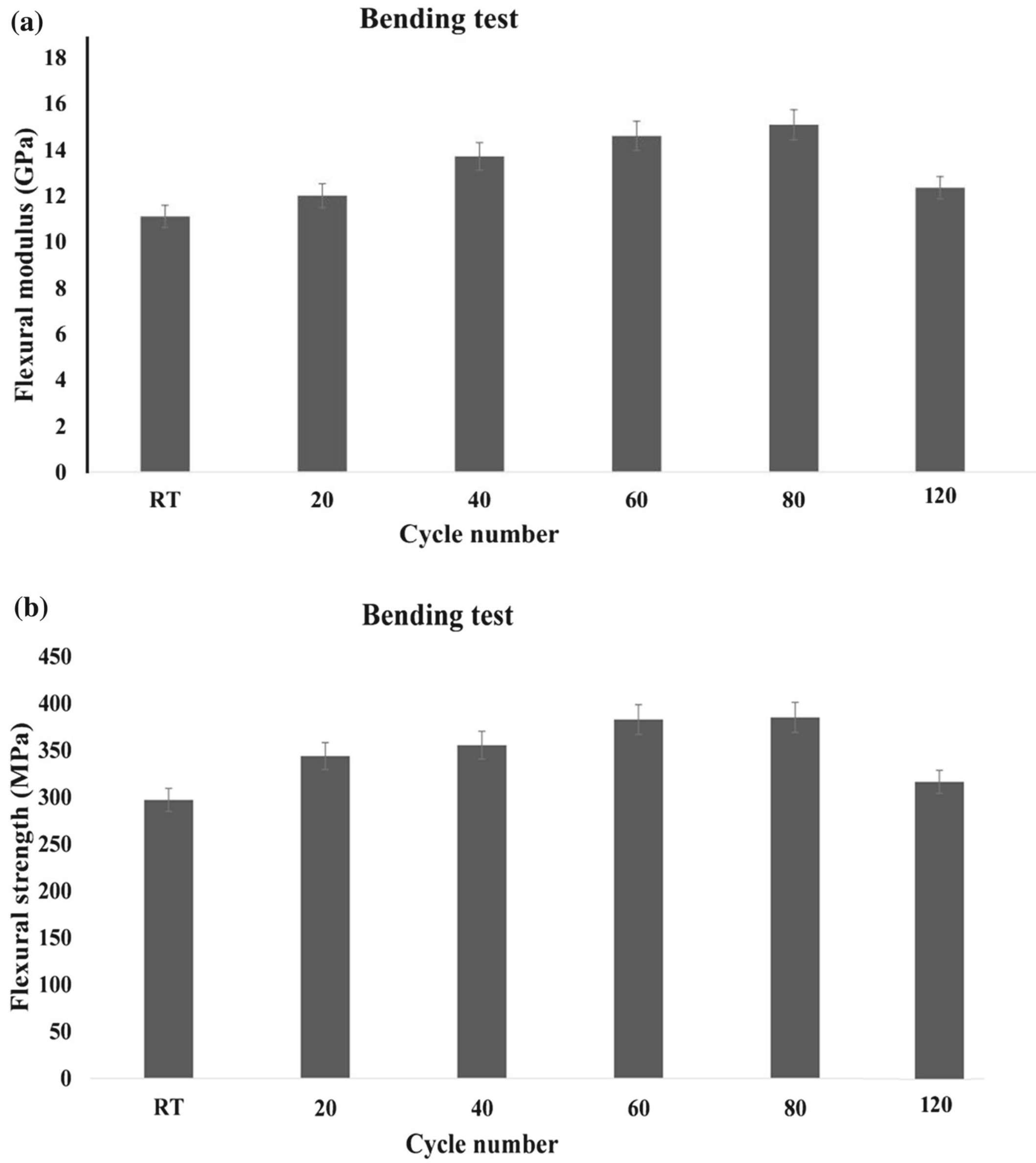

Figure 5. (**a**) Flexural modulus and (**b**) flexural strength of BFRP composites before and after various numbers of thermal cycling exposure.

composites were determined using tensile, bending and SBS experiments.

3.1a *Tensile test*: Figure 4 shows a comparison between modulus of elasticity (figure 4a) and tensile strength (figure 4b) of BFRP composites before and after thermal cycling. As mentioned, two phenomena may have occurred during thermal cycling. Post curing process improved mechanical properties of composite material by increasing crosslink. The increase in temperature after postcuring, created a mismatch between fibres and matrix due to a difference in their CTEs. The modulus of elasticity and tensile strength of original BFRP composite increased approximately by 9.5% when it was exposed to 20 cycles between −40 and +120°C. The dominant effects of possible post-curing process, which occurred during thermal cycling, had a key role on this increase. The temperature during thermal cycling was not high enough to break the chemical bonds and crosslinks between basalt fibres and epoxy [51]. The post-curing effects increased the modulus of elasticity by 1.5, 2 and 2% after 40, 60 and 80 number of cycles, respectively. Moreover, the modulus of elasticity decreased by 13% after 120 cycles. The tensile strength similar to modulus of elasticity increased by 11.2, 13.4 and 15.8% after above mentioned cycle numbers and it decreased by 11% after 120 cycles. Generally, thermal treatment affects the polymerbased composite materials differently based on the type of polymer and their chemical structure. On the other hand, the time of thermal treatment

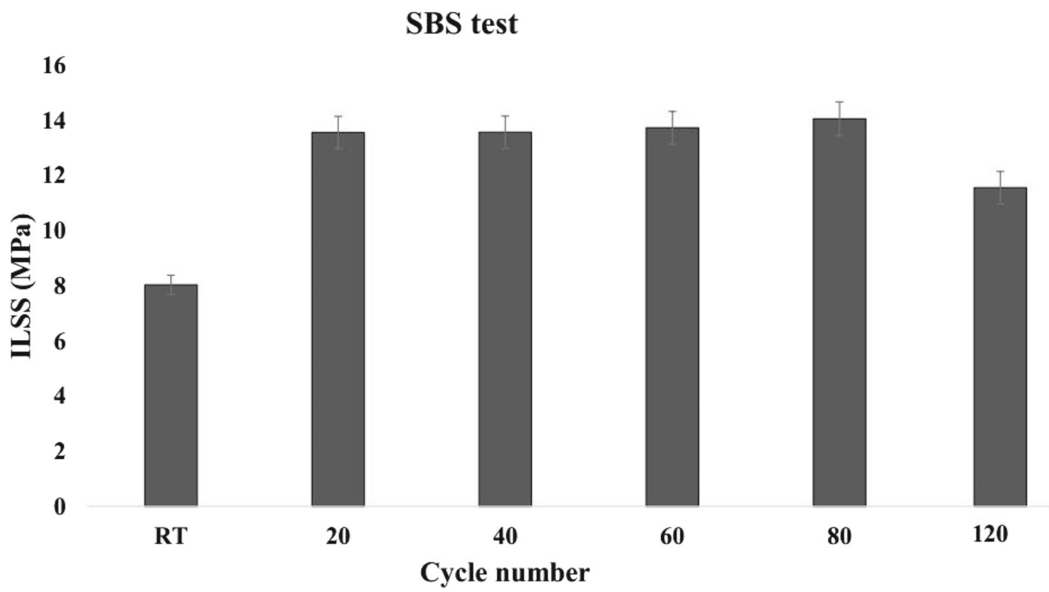

Figure 6. ILSS of BFRP composites before and after thermal cycling exposure.

is one of the most important factors which may provide inconsistent effects in the structure of composite especially in the interface of fibre and matrix. Increasing the cycle numbers at the beginning of thermal cycling leads to the improvement of mechanical properties of composites. This phenomenon occurs due to the post-curing in the structure of epoxy and enhancement of cross-links at the interface of the fibres and matrix. Increasing the cycle numbers also leads to mismatch in the interface of the composite due to different coefficients of thermal expansion between the composite components. Moreover, microcracks will be initiated with the increase in cycle numbers and therefore, long cracks are created with joining of such microcracks. Finally, with delamination forming in the structure of the composite, the mechanical properties of the polymer composites are decreased. In our study, due to characteristics of epoxy resin, especially structure of basalt fibres and their superior strength against high temperatures, first, the mechanical properties of composite are improved by the increase in cycle numbers up to 100 cycles. However, after 100 cycles, the debonding due to mismatch of thermal expansion coefficient weakened the composite structure and reduced the mechanical properties. Given the standard deviation in the tensile strength, there is no significant increase in tensile strength in 20, 40, 60 and 80 thermal cycles (figure 4b).

3.1b *Bending test*: Figure 5 shows the flexural properties of BFRP composites before and after thermal cycling. As seen in figure 5a and b, the flexural modulus and strength of BFRP composites increased from 11.1 GPa and 297 MPa to 12 GPa and 343 MPa after 20 cycles and reached to 13.7 GPa and 355.5 MPa after 40 cycles, respectively. This trend was continued until the flexural modulus and strength of BFRP reached 15.1 GPa and 385 MPa after 80 cycles. Such phenomena happened due to postcuring strengthening effect and strong bonds development between basalt fibres and epoxy matrix. It is worth mentioning that the temperature was not high enough to break the chemical bonds at the interface [52,53]. Also, the increase of flexural properties between 60 and 80 cycles was not significant. It is important to note that the flexural modulus and strength of BFRP composites significantly decreased when the number of cycles reached 120.

3.1c *SBS test*: Figure 6 shows a comparison between ILSS results of BFRP composites before and after thermal cycling. As is evident in figure 6, the amount of ILSS for original BFRP composite is about 8.0 MPa. By increasing the cycles to 20, this amount also increased by 68.8%. The increase of ILSS value possibly occurred because of the polymerization that happened by post-curing. The increase in crosslinks between fibres and matrix improved shear strength of composites. By increasing the cycles, the effect of post-curing subsided and ILSS value was not affected by thermal cycling up to 40 cycles. After 40 cycles, ILSS increased slightly and this increase continued up to 80 cycles when ILSS reached its highest amount (14.1 MPa) at 80 cycles. Considering the standard deviation, the increase in ILSS between 20 and 80 cycles is not very noticeable. Finally, the ILSS value was significantly decreased when the number of cycles reached 120. As discussed earlier, by increasing the number of cycles over 100, the debonding weakened the composite structure because of mismatch of thermal expansion coefficient and reduced the mechanical properties of tested specimens.

3.2 *Thermal test (DMA)*

Viscoelastic properties of original and thermal cycling exposure BFRP samples were determined using dynamic

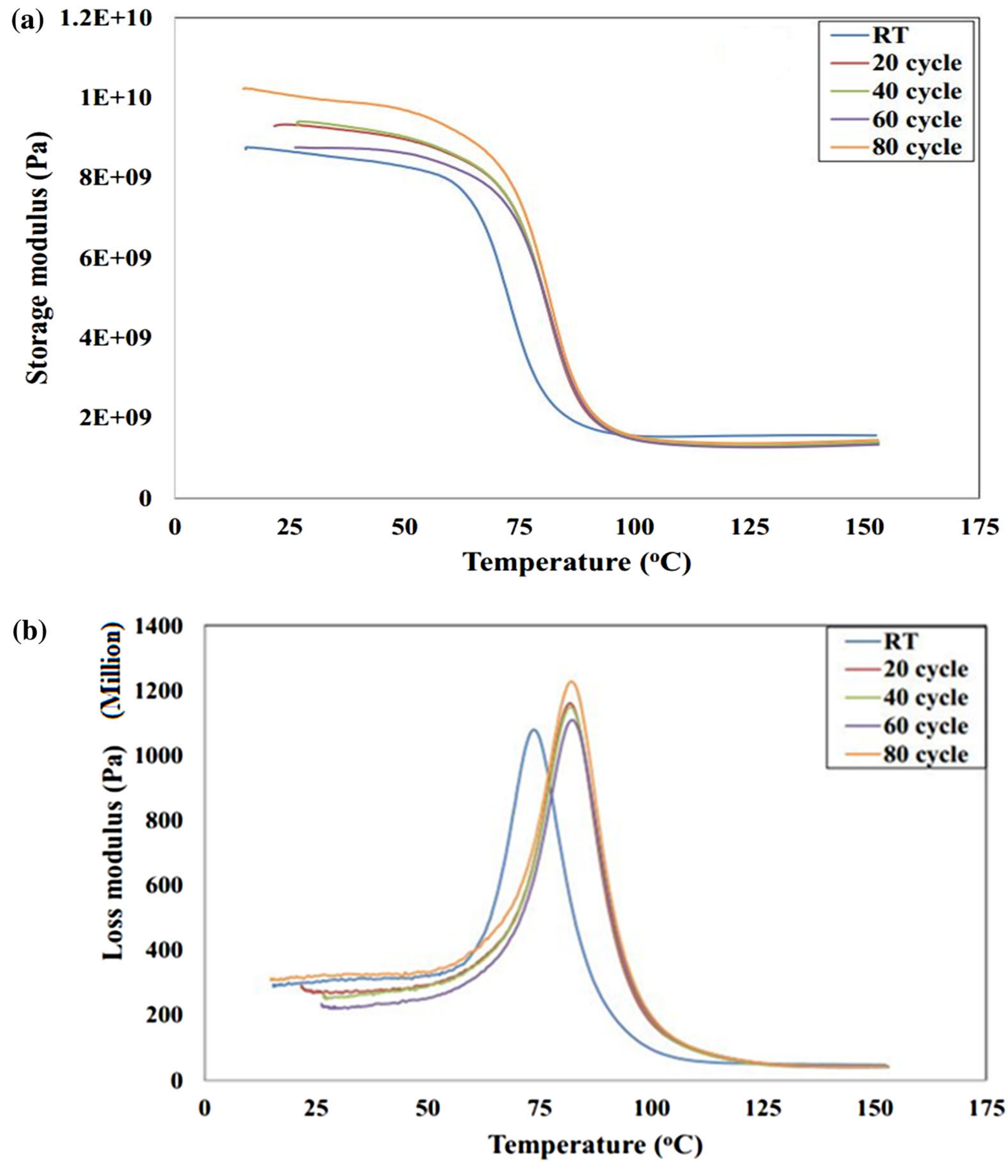

Figure 7. (**a**) Storage modulus (E') and (**b**) loss modulus (E'') *vs.* temperature for original and thermal exposure BFRP samples.

mechanical analysis experiment. Figure 7a and b shows the storage modulus (E'), loss modulus (E'') *vs.* temperature for BFRP.

The composite was exposed to DMA experiment to test three states i.e. glassy state, glass transition state and rubbery state. In the glassy state, the segmental mobility in the structure of material was limited and the material had the highest storage modulus value [46]. In the glass transition state, the storage modulus was decreased sharply by a slight change in temperature. Glass transition temperature which was the most important characteristic of polymeric composites was determined by analysing the transition region. Thus, this state gained high importance for characterization of the viscoelastic properties of polymer composites. No significant change in the storage modulus was occurred in the rubbery state [54]. As seen in figure 7a, the sample exposed to 80 cycles, gained the highest amount of storage modulus value in the glassy state. The values of glass transition temperature (T_g) and the maximum tan δ values of the BFRP composites were extracted from the DMA traces which has been illustrated in table 3. It was evident that the T_g and tan δ values for the original samples were lower than those for tested specimens. On the other hand, the sample exposed to 80 cycles gained the highest T_g value. This observation was similar to the results of mechanical tests in which the sample was exposed to 80 cycles and gained the highest tensile strength, flexural modulus and ILSS. This may be caused by further crosslinking effect due to the high temperature [54,55].

Table 3. Glass transition temperature and damping factors of RT and thermal exposure BFRP composites.

Material	tan δ_{max}	T_g
RT	0.2749	77.064
20 cycle exposed	0.3153	85.82
40 cycle exposed	0.3100	86.09
60 cycle exposed	0.3097	86.10
80 cycle exposed	0.3180	86.18

Table 4. Contact angle and nature of RT and thermal cycling exposure BFRP composite materials.

Samples	Contact angle (°)	Nature
RT	69.58	Hydrophil
20 cycle exposure	68.23	Hydrophil
40 cycle exposure	65.66	Hydrophil
60 cycle exposure	63.12	Hydrophil
80 cycle exposure	61.31	Hydrophil

3.3 *Hydrophobicity test*

The hydrophobicity test results of original and thermal cycle exposure BFRP composites were illustrated in table 4. According to test results, the contact angle of original BFRP was 69.6, which showed that the BFRP was from hydrophobic type material. This occurred due to hydrophobic nature of basalt fibre. It was observed that by increasing the number of cycles from 20 to 80 cycles, the contact angle of BFRP samples was slightly reduced and the water absorption quality of samples was enhanced. The test results showed that the thermal cycling process not only was able to change the water absorption nature of BFRP composites, but it also intensified its hydrophilic nature. When the temperature is increased, the evaporation rate also increased. Therefore, the hydrophilic nature of the composite increased.

3.4 *Fracture surfaces*

SEM with a FEI Quanta 200 FEG environmental scanning electron microscope was used to see fracture surfaces. A small section of crosssection of composite laminates exposed to tensile test after thermal cycling was prepared for SEM observation. As shown in figure 8, different failure modes were observed in tested specimens. The fracture surface showed a macroscopic brittle character. According to figure 8a, SEM micrograph of tensile fracture surface at crack origin (region), a set of fibre bundles was broken. Such cracks were created during deformation due to the temperature variation and different behaviours of matrix and fibre. These phenomena acted as stress concentrator to initiate and propagate cracks under tensile loading. According to fracture surface, as shown in figure 8b, the fibre pull out and bundle breakage were the dominant modes for the fracture in tensiletested specimens.

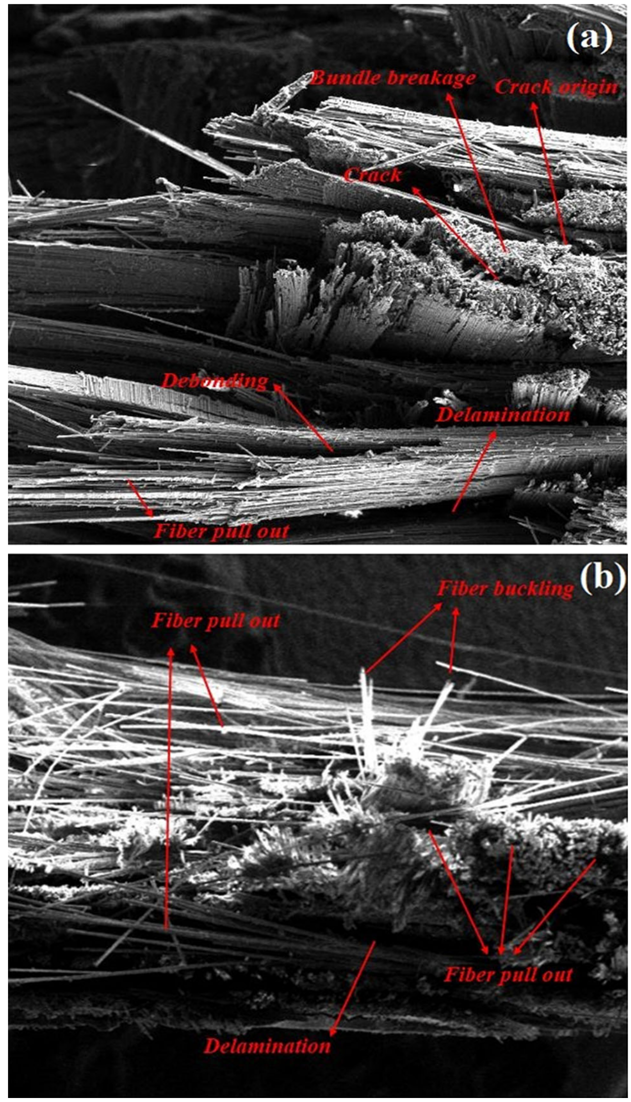

Figure 8. SEM micrographs of fracture surfaces of (**a**) tensile and (**b**) bending tested specimens.

4. Conclusion

In this study, the effect of thermal cycling on mechanical and thermal properties of basalt fibre-reinforced epoxy matrix composites was investigated. In this survey, the mechanical properties of original and thermal cycling BFRP composites, such as tensile strength, flexural modulus and ILSS were extracted using tensile, bending and SBS tests. DMA test was employed to examine the thermal properties of composites. Therefore, viscoelastic properties, such as storage modulus and glass transition temperature of original and thermal-treated BFRP composites were compared. The results showed that the thermal cycling affected the mechanical and thermal properties of BFRP composites by post-curing. This was a result of high temperature process, which led to polymerization and increasing crosslinks at the interface of composite and it improved the mechanical and viscoelastic properties of BFRPs. The other effect of thermal cycling process was degradation of mechanical properties caused by residual thermal stress due to mismatch in CTE of composite components. Such mismatch also led to stress concentration at the interface of composite, creation of cracks and delamination in the region. It was concluded that number of cycles did not affect the mechanical and thermal properties of BFRPs significantly. The hydrophobicity test results illustrated that the original BFRP composites were from hydrophilic type materials because their hydrophilic nature increased by increasing the number of cycles during thermal cycling. According to SEM micrographs, debonding and delamination, which caused by the thermal cycling, and the fibre pull out, fibre breakage and fibre buckling caused by mechanical loading, were the most important fracture modes in composite materials.

References

[1] Saheb D N and Jog J P 1999 *Adv. Polym. Tech.* **18** 351
[2] Lee J H, Rhee K Y and Park S J 2010 *Mater. Sci. Eng. A* **527** 6838
[3] Kalam A, Saharib B B, Khalid Y A and Wong S V 2005 *Compos. Struct.* **71** 34
[4] Artemenko S E and Kadykova Y A 2008 *Fibre Chem*. **40** 37
[5] Dai J, Pellaton D and Hahn H T 2003 *Polym. Compos.* **24** 672
[6] Dong C, Ranaweera-Jayawardena H A and Davies I J 2012 *Compos. Part B* **43** 573
[7] Wei B, Cao H L and Song S H 2011 *Corros. Sci.* **53** 426
[8] Czigany T 2006 *Compos. Sci. Tech.* **66** 3210
[9] Liu Q, Shaw M T, Parnas R S and McDonell A M 2006 *Polym. Compos*. **27** 475
[10] Rout J, Misra M, Tripathy S S, Nayak S K and Mohanty A K 2011 *Compos. Sci. Tech.* **61** 1303
[11] Alavudeen A, Rajini N, Karthikeyan S, Thiruchitrambalam M and Venkateshwaren N 2015 *Mater. Des.* **66** 246
[12] Carmisciano S, De Rosa I M, Sarasini F, Tamburrano A and Valente M 2011 *Mater. Des.* **32** 337
[13] Nayak S K, Mohanty S and Samal S K 2009 *Mater. Sci. Eng. A* **523** 32
[14] Silva R V, Aquino E M F, Rodrigues L P S and Barros A R F 2009 *J. Reinf. Plast. Compos.* **28** 1857
[15] Demir H, Atikler U, Balköse D and Tıhmınlıoğlu F 2006 *Compos. Part A: Appl. S. Man.* **37** 447
[16] Zhong L X, Fu S Y, Zhou X S and Zhan H Y 2011 *Compos. Part A: Appl. S. Man.* **42** 244
[17] Sarasini F, Tirillò J, Valente M, Ferrante L, Cioffi S, Iannace S *et al* 2013 *Mater. Des*. **49** 290
[18] Szabo J S and Czigany T 2003 *Polym. Test.* **22** 711
[19] Zhang H, Zhang Z and Breidt C 2004 *Compos. Sci. Tech.* **64** 2021
[20] Dhand V, Mittal G, Rhee K Y, Park S J and Hui D 2015 *Compos. Part B Eng.* **73** 166
[21] Quagliarini E, Monni F, Lenci S and Bondioli F 2012 *Construct. Build. Mater.* **34** 372
[22] Zhang L, Du W, Nautiyal A, Liu Z and Zhang X 2018 *Sci. China Mater.* **61** 303
[23] Lobanov D S and Slovikov S V 2018 *Mech. Compos. Mater*. **54** 351
[24] Ramachandran B E, Velpari V and Balasubramanian N 1981 *J. Mater. Sci.* **16** 3393
[25] Sim J, Park C and Moon D Y 2005 *Compos. Part B Eng.* **36** 504
[26] Fiore V, Di Bella G and Valenza A 2011 *Mater. Des.* **32** 2091
[27] Fiore V, Scalici T, Di Bella G and Valenza A 2015 *Compos. Part B Eng.* **74** 74
[28] Wei B, Cao H L and Song S H 2010 *Mater. Des.* **31** 4244
[29] Lu Z, Xian G and Li H 2016 *Construct. Build. Mater.* **127** 1029
[30] Qiang L, Montgomery T S and Parnas R S 2006 *Polym. Compos*. **27** 475
[31] Botev M, Betchev H, Bikiaris D and Panayiotou C 1999 *J. Appl. Polym. Sci.* **74** 523
[32] Chandekar G S and Kelkar A D 2014 *Sci. World. J.* **2014** 1
[33] Tehrani-Dehkordi M, Nosraty H and Rajabzadeh M H 2015 *Fiber. Polym.* **16** 918
[34] Lopresto V, Leone C and De Iorio I 2011 *Compos. Part B* **42** 717
[35] Zhang Y, Yu C, Chu P K, Lv F, Zhang C, Ji J *et al* H 2012 *Mater. Chem. Phys.* **133** 845
[36] Azimpour Shishevan F and Akbulut H 2019 *Iran J. Sci. Tech. Trans. Mech. Eng.* **43** 225
[37] Kim H 2012 *Fiber. Polym.* **13** 762
[38] Kim H 2014 *Fiber. Polym.* **14** 1311
[39] Liu Q, Shaw M T, Parnas R S and McDonnel A M 2006 *Polym. Compos*. **27** 41
[40] Azimpour F, Akbulut H and Mohtadi-Bonab M A 2017 *J. Mater. Eng. Perform.* **26** 2890
[41] Ray B C 2006 *J. Appl. Polym. Sci.* **100** 2062
[42] He J, Shi J, Cao X and Hu Y 2018 *Adv. Civil Eng*. **2018** 1
[43] Mikata Y and Taya M 1985 *J. Comp. Mat.* **19** 554
[44] Azimpour-Shishevan F, Akbulut H and Mohtadi-Bonab M A 2019 *J. Dyn. Behav. Mater.* **5** 161
[45] Kmita G, Nowak T and Sekula R 2012 *Appl. Compos. Mater*. **19** 65
[46] Chu Y H, Fu Q, Li H and Li K 2011 J. *Alloys Compd.* **509** 8111
[47] Wei L, Zhenhu C, Ding C, Cang F and Canrang W 2010 *J. Alloys Compd.* **504** 522
[48] Ramanujam N, Vaddadi P, Nakamura T and Singh R P 2008 *Compos. Struct*. **85** 175
[49] Asp L E, Berglund L A and Talreja R 1996 *Compos. Sci. Tech.* **56** 1089
[50] Ronga M Z, Zhang M Q and Liu Y 2006 *Compos. Sci. Tech*. **61** 1437
[51] Eslami-Farsani R, Khalili S M R and Najafi M 2013 *J. Therm. Str*. **36** 684
[52] Griffiths R and Ball A 2000 *Compos. Sci. Tech.* **60** 2747
[53] Segovia F, Ferrer C, Salvador M D and Amigó V 2001 *Polym. Degrad. Stabil.* **71** 179
[54] Komalan C, George K E, Kumar P A S and Varughese K 2007 *Exp. Polym. Let.* **1** 641
[55] Yu Q, Chen P, Gao Y, Mu J, Chen Y, Lu C *et al* 2011 *Mater. Chem. Phys.* **130** 1046